



# Incorporating topological derivatives into level set methods

Martin Burger<sup>a,\*</sup>, Benjamin Hackl<sup>b</sup>, Wolfgang Ring<sup>c</sup>

<sup>a</sup> *Department of Mathematics, University of California, 520 Portola Plaza, Los Angeles, CA 90095-1555, USA*

<sup>b</sup> *SBF F 013, Numerical and Symbolic Scientific Computing, Freistädterstr. 313, A-4040 Linz, Austria*

<sup>c</sup> *Department of Mathematics, University Graz, Heinrichstr. 36, A-8010 Graz, Austria*

Received 24 July 2003; accepted 16 September 2003

---

## Abstract

The aim of this paper is to investigate the use of topological derivatives in combination with the level set method for shape reconstruction and optimization problems. We propose a new approach generalizing the standard speed method, which is obtained by using a source term in the level set equation that depends on the topological derivative of the objective functional. The resulting approach can be interpreted as a generalized fixed-point iteration for the optimality system (with respect to topological and shape variations). Moreover, we apply the new approach for a simple model problem in shape reconstruction, where the topological derivative can be computed without additional effort. Finally, we present numerical tests related to this model problem, which demonstrate that the new method based on shape and topological derivative successfully reconstructs obstacles in situations where the standard level set approach fails.

© 2003 Elsevier B.V. All rights reserved.

*PACS:* 02.30.Zz; 02.60.Pn; 02.60.Lj

*Keywords:* Level set method; Topology optimization; Shape reconstruction; Shape derivative; Topological derivative; Hamilton–Jacobi equations

---

## 1. Introduction

Topology optimization or shape reconstruction with unknown a-priori knowledge of the topological structure of the solution is an important task in applications and a great challenge. In the context of topology optimization the problem of changing topologies can sometimes be circumvented by using homogenization approaches (cf. [2,6]), which, however, suffer from several limitations. In particular homogenization is restricted to special classes of objective functionals and has difficulties to handle complex physical situations such as design-dependent loads (cf. [7]). An attractive alternative to solve the original

---

\* Corresponding author.

*E-mail addresses:* [martin.burger@jku.at](mailto:martin.burger@jku.at) (M. Burger), [hackl@sfb013.uni-linz.ac.at](mailto:hackl@sfb013.uni-linz.ac.at) (B. Hackl), [wolfgang.ring@uni-graz.ac.at](mailto:wolfgang.ring@uni-graz.ac.at) (W. Ring).

<sup>1</sup> On leave from: Industrial Mathematics Institute, Johannes Kepler Universität, A 4040 Linz, Austria.

problem without homogenization are level set methods, originally introduced by Osher and Sethian [23], which allow to handle certain types of topological changes in an automatic way.

For several optimization problems, the level set method was successfully applied to compute optimal geometries without a-priori knowledge of the number of connected components (cf. [8,9,11,12,17–19,21,22,25]). In some applications to structural design it was observed that a level set approach may get stuck at shapes with less holes than the optimal geometry (cf. [3,4]), i.e., the method encounters severe problems to create new holes. Another example of the stopping of a level set method in a nonoptimal shape in the context of shape reconstruction will be presented in Section 3. In all these examples, the choice of the normal velocity for the evolving level sets was based on the shape gradient of a given functional, which can be obtained using e.g. the speed method from classical shape optimization (cf. [29,31]).

The aim of this paper is to generalize the level set approaches for shape optimization and reconstruction by including the *topological derivative* (cf. [27,28]), which is related to changes in the objective functional corresponding to the introduction of (infinitesimally) small holes. We propose a genuine modification of the level set approach in this case and demonstrate the success of the modified level set approach in some numerical examples, where the standard level set approach does not yield optimal shapes.

The model problem we investigate here consists in the minimization of the least-squares functional

$$J(\Omega) = \frac{1}{2} \int_D |u - u^*|^2 dx, \quad (1)$$

over the set  $\mathcal{K}(D)$  of all compact subsets of  $D$ , where the relation between  $u$  and the shape  $\Omega$  is given by the elliptic partial differential equation

$$-\Delta u = f_\Omega, \quad (2)$$

subject to homogeneous Dirichlet boundary conditions on  $\partial D$ . Here  $f_\Omega$  denotes the characteristic function of the shape  $\Omega$ , i.e.,

$$f_\Omega(x) = \begin{cases} 1 & \text{if } x \in \Omega, \\ 0 & \text{else.} \end{cases} \quad (3)$$

Due to the paper's focus on the incorporation of the topological derivative into level set approaches for shape reconstruction, we do not treat other important issues of these problems such as regularization in presence of noise or the discretization of the state, adjoint, and level set equation.

The paper is organized as follows: First we introduce the shape and topological derivatives in Section 2, which are the main tools used in the following. Next we give a short introduction to level set methods in Section 3. Motivated by the interpretation of the topological derivative we suggest a modification of the level set method that incorporates the topological derivative in Section 4. Finally, in Section 5, we present the results of some numerical experiments for our model problem.

## 2. Shape and topological derivatives

In this section, we shall define two different types of perturbations of a shape variable and we shall present concepts for sensitivity calculations of a given shape functional with respect to the considered perturbations. The first type of perturbations is concerned with variations of the boundary of the shape along a given speed vector field  $V$ . The derivative of a given function  $y = y(\Omega)$  with respect to a perturbation defined by the vector field  $V$  is called the *shape derivative*  $y'(\Omega; V)$  of  $y$  at  $\Omega$  in direction of  $V$ . The shape derivative  $J'(\Omega; V)$  of a *functional*  $J : \mathcal{O} \rightarrow \mathbb{R}$  with respect a perturbation defined by the vector field  $V$  is sometimes called the Eulerian derivative of  $J$  at  $\Omega$  in the direction  $V$ . Here  $\mathcal{O}$  is an appropriate set of

shapes. For a comprehensive introduction to this topic we refer to the monographs by Sokolowski and Zolésio [29] and by Delfour and Zolésio [10].

Looking at the shape from a global viewpoint, variations of the existing shape boundaries are only one possibility. Another obvious one consists in perturbing the global shape by changing its topology. This idea is fundamental for the so-called *topological derivative*, which is based on the variation of  $J(\Omega)$  with respect to small holes at a certain position  $x \in \Omega$ . The respective derivative is denoted by  $d_{\mathcal{F}}J(\Omega)(x)$ . For an application to topology optimization we refer to Schumacher [26] and for the calculation of topological derivatives for elasticity problems we refer to Sokolowski and Żochowski [27,28]. A related approach is the topological asymptotic recently used by Guillaume et al. [13,15].

In the following we shall give a short introduction to the concepts of *shape derivative* and *topological derivative* and we shall calculate both derivatives for our model example (2). The derivatives will be needed in Section 4.

### 2.1. Shape derivatives

Assume that we are considering a class of shapes  $\mathcal{O} \subset 2^{\mathbb{R}^N}$ . For  $\Omega \in \mathcal{O}$  and a vector field  $V : \mathbb{R}^N \rightarrow \mathbb{R}^N$  we define perturbations  $\Omega_t$  of  $\Omega$  of the form

$$\Omega_t(V) = \{T_t(\mathbf{x}, V) : \mathbf{x} \in \Omega\},$$

where  $T_t(\cdot, V)$  is the solution map (the flow) with respect to the dynamical system

$$\mathbf{x}' = V(\mathbf{x}), \tag{4}$$

i.e.,  $T_t(\mathbf{x}, V)$  is the solution to (4) at time  $t$  with initial value (at time 0) given by  $\mathbf{x}$ .

For an operator  $\mathcal{F} : \mathcal{O} \rightarrow \mathcal{X}$  (with values in some vector space  $\mathcal{X}$ ), we compute (formally) the shape derivative of  $\mathcal{F}$  as

$$\mathcal{F}'(\Omega)[V] = \left. \frac{d}{dt} (\mathcal{F}(\Omega_t(V))) \right|_{t=0}.$$

It can be shown [10] that the shape derivative depends only on  $V|_{\Gamma}$ , where  $\Gamma = \partial\Omega$ . For smooth shapes, the perturbation vector field can be decomposed into a normal and a tangential component on  $\Gamma$ . The flow with respect to the tangential component leaves  $\Omega$  invariant. Therefore, the shape derivative is independent of the tangential component and we obtain

$$\mathcal{F}'(\Omega)[V] = \mathcal{F}'(\Omega)[v\mathbf{n}],$$

where  $v = V \cdot \mathbf{n}$  with  $\mathbf{n}$  denoting the exterior unit normal vector field on  $\Gamma$ . Hence, it is sufficient to consider only normal perturbation fields which are defined by the corresponding scalar function  $v$ .

For shape optimization problems, we are interested in finding a direction of perturbation  $v$  for which the value of the given shape functional  $J(\Omega)$  decreases most rapidly. If the action of the shape derivative in direction of a perturbation  $v$  is written as a linear form  $\langle g, v \rangle_{B',B}$  where  $B$  is an appropriate Banach space of function on  $\Gamma$  and  $B'$  is its dual, then the direction of steepest descent with respect to the shape functional  $J$  is given by  $v = -j(g)$ , where  $j : B' \rightarrow B$  denotes the duality mapping. By extending shape derivatives to less smooth shapes and variations (which is possible for many examples), the velocity method can be used in combination with level set methods, to define level set evolutions with decreasing objective function values.

It can be proved that the shape derivative of the objective function (1) under the constraints (2) and (3) is given by

$$J'(\Omega)[V] = \int_D (u(\Omega) - u^*)u'(\Omega)[V] \, dx,$$

where the shape derivative  $u'$  is characterized in the following theorem (cf. [16]).

**Theorem 2.1.** *Let  $\Omega \subset D$  be a domain with boundary  $\partial\Omega$  in the class  $C^1$ , and let  $V \in C^1(\mathbb{R}^N, \mathbb{R}^N)$  be the velocity field that determines the evolution of  $\Omega$ . Then the map  $u(\Omega) : \mathcal{O} \rightarrow H_0^1(D)$  maps  $\Omega$  onto the solution  $u(\Omega)$  of (2), has a shape derivative  $u' \in H_0^1(D)$  that is given as the solution to*

$$\begin{aligned} -\Delta u' &= 0 \quad \text{in } \Omega \cup (D - \overline{\Omega}), \\ \llbracket \frac{\partial u'}{\partial n} \rrbracket &= V \cdot n \quad \text{on } \partial\Omega. \end{aligned} \tag{5}$$

Here  $\llbracket h \rrbracket$  denotes the jump of a function  $h$  across the interface  $\partial\Omega$ .

Defining  $w \in H_0^1(\Omega)$  as the unique solution of the adjoint problem

$$\int_D \nabla w \cdot \nabla h \, dx = \int_D (u(\Omega) - u^*)h \, dx \quad \forall h \in H_0^1(D), \tag{6}$$

we can write the shape derivative of  $J(\Omega)$  in the standard form:

$$J'(\Omega)[V] = \int_{\partial\Omega} wV \cdot \mathbf{n} \, ds. \tag{7}$$

### 2.2. Topological derivatives

While the shape derivative is based on local perturbations of the boundary of the domain  $\Omega$  (continuous perturbations with respect to the Hausdorff distance), the *topological derivative* measures the influence of small holes (topology changes) in  $\Omega$ . Such perturbations are continuous in the  $L^1$ -distance of sets. Again we consider a map  $\mathcal{F} : \mathcal{O} \rightarrow \mathcal{X}$  where  $\mathcal{X}$  may equal  $\mathbb{R}$  or a suitable Banach space. Then the topological derivative is defined via

$$d_{\mathcal{F}} \mathcal{F}(\Omega)(x) := \lim_{\rho \rightarrow 0} \frac{\mathcal{F}(\Omega_{\rho,x}) - \mathcal{F}(\Omega)}{|B_{\rho,x} \cap \Omega|} \quad \forall x \in \overline{\Omega}, \tag{8}$$

where  $B_{\rho,x} = \{y \in \mathbb{R}^d \mid |y - x| < \rho\}$ ,  $\Omega_{\rho,x} = \Omega - \overline{B_{\rho,x}}$  and  $|A|$  denotes the Lebesgue measure of the set  $A$ .

If  $\mathcal{F}$  is some objective function to be minimized, the topological derivative provides information where to place holes such that the objective function is reduced. This complements the information of the shape derivative which tells how to evolve the existing shape, but not how to introduce new shapes, to achieve a reduction of the objective function.

Originally the topological derivative was intended to subtract material at  $x \in \Omega$ , but in some applications, especially in our application, it makes also sense to add material at  $x \in D - \Omega$ . In this case the “set-minus” must be replaced by “union” in (8). For the sake of simplicity, we treat only one of the possible two case (the “set-minus” case) thoroughly and deal with the other case by analogy.

In the following we calculate the topological derivative for the objective  $J(\Omega)$  defined in (1). During the derivation we will often need the expressions  $u(\Omega)$ ,  $u(\Omega_{\rho,x})$ , which we denoted in the following by  $u, u_{\rho,x}$ . We start with a proposition on the expansion of the state  $u$  with respect to a perturbation of radius  $\rho$ :

**Proposition 2.2.** Let  $\Omega \subset D$  be some measurable domain with positive measure and  $u_{\rho,x}, u$  be the corresponding solutions to the Dirichlet problem for (2), then there exists a constant  $C > 0$  such that

$$\|u_{\rho,x} - u\|_{H^1(D)} \leq C|B_{\rho,x} \cap \Omega|^{\frac{1}{q}}, \tag{9}$$

where  $q \in ]\frac{2d}{d+2}, \infty]$

**Proof.** The difference between the solutions satisfies

$$-\Delta(u_{\rho,x} - u) = f_{\Omega_{\rho,x}} - f_{\Omega},$$

and hence, by a standard stability estimate we obtain that

$$\|u_{\rho,x} - u\|_{H^1(D)} \leq C_0 \|f_{\Omega_{\rho,x}} - f_{\Omega}\|_{H^{-1}(D)}$$

for some constant  $C_0$ . The assertion follows now from the continuous embedding of  $H^{-1}(D)$  into  $L^q(D)$  [1] and the fact that

$$\|f_{\Omega_{\rho,x}} - f_{\Omega}\|_{L^q(D)} = \left( \int_{B_{\rho,x} \cap \Omega} 1 \, dx \right)^{\frac{1}{q}}.$$

Note that with additional regularity results for (2) even stronger results than in Proposition 2.2 could be obtained for smooth data.  $\square$

**Theorem 2.3.** Let  $\Omega \subset D$  be some measurable domain with positive measure,  $J(\Omega)$  be the objective function defined in (1) and  $w$  be the solution to the adjoint problem (6). Then the topological derivative  $d_{\mathcal{T}}J(\Omega)(x)$  is given by

$$d_{\mathcal{T}}J(\Omega)(x) = \begin{cases} -w(x) & x \in \overline{\Omega} \\ w(x) & x \in D - \overline{\Omega} \end{cases} \text{ a.e.} \tag{10}$$

**Proof.** We only proof the assertion in the case  $x \in \overline{\Omega}$ , that is, we subtract a material. The second case  $x \in D - \overline{\Omega}$  can be treated analogously. Note that the case where we add or subtract material locally in a neighborhood of a point  $x \in \partial\Omega$  corresponds to a local perturbation of the boundary and is treated within the concept of shape derivative in Section 2.1.

- To calculate the limit in (8) we have to consider the difference

$$J(\Omega_{\rho,x}) - J(\Omega) = \frac{1}{2} \int_D (u_{\rho,x} - u)^2 \, dx - \int_D (u_{\rho,x} - u)(u - u^*) \, dx.$$

- We can estimate the first term by

$$\|u_{\rho,x} - u\|_{L_2(D)}^2 \leq O(|B_{\rho,x} \cap \Omega|^{\frac{2}{q}}),$$

where we choose  $q < 2$  which is possible due to Proposition 2.2. Hence the limit  $\rho \rightarrow 0$  of this term divided by  $|B_{\rho,x} \cap \Omega|$  tends to zero.

- The second term can be rewritten, using the definition of the adjoint problem (6), as

$$\int_D (u_{\rho,x} - u)(u - u^*) \, dx = \int_D \nabla(u_{\rho,x} - u) \cdot \nabla w \, dx = \int_D (f_{\Omega_{\rho,x}} - f_{\Omega})w \, dx = - \int_{B_{\rho,x} \cap \Omega} w \, dx.$$

- With the Lebesgue-differentiation-theorem [14] the limit of the second term divided by  $|B_{\rho,x} \cap \Omega|$  is almost everywhere given by

$$\lim_{\rho \rightarrow 0} \frac{1}{|B_{\rho,x} \cap \Omega|} \int_{B_{\rho,x} \cap \Omega} w \, dx = w(x),$$

which completes the proof.  $\square$

A closer look at the proof of Theorem 2.3 shows that along the same lines more complicated objective functions and even more complicated problems like inclusion detection problems can be treated as soon as one has an estimate like in Proposition 2.2.

One observes that the topological derivative can be computed without any additional effort if we have already computed the shape derivative in this example. This statement is not true in general, but one can still use the adjoint method to compute the topological derivative with similar effort as the shape derivative. For the computation of topological derivatives for other interesting problems like inclusion detection and structural shape optimization we refer to Sokolowski and Żochowski [27,28].

### 3. Connecting level set and speed methods

We already mentioned in Section 2.1 that the shape derivative provides information of how to evolve a given shape such that the objective function (1) decreases during the evolution. The problem is now to represent and evolve a shape in a suitable way. One of the possible techniques is the *level set method*.

The key feature of the level set approach is to represent domains and their boundaries not via parameterizations, but as level sets of a continuous function  $\phi$ , the so-called level set function.

For the computation of an evolving open set  $\Omega(t)$ ,  $t \in \mathbb{R}^+$ , one can assume that the level set function  $\phi$  on  $\mathbb{R}^N \times \mathbb{R}_+$  is time-dependent. Assuming this, the evolution of  $\Omega_t$  is alternatively determined by the evolution of the level set function, where the connection between evolving shape and evolving level set function is established via

$$\Omega(t) = \{\phi(\cdot, t) < 0\}.$$

The boundary  $\Gamma(t)$  of  $\Omega(t)$  (if  $\phi(\cdot, t)$  vanishes only on a set of Lebesgue measure zero) is then given by the zero-level set, i.e.,

$$\Gamma(t) = \{\phi(\cdot, t) = 0\}.$$

Suppose that the evolution of the shape is determined by a flow  $x(t) = T_t(\mathbf{x}, V)$  such that

$$\frac{dx}{dt}(t) = V(x(t)),$$

as described in Section 2.1. Then the corresponding evolution of the level set function  $\phi$  is determined by the first-order transport equation

$$\frac{\partial \phi}{\partial t} + V \cdot \nabla \phi = 0, \quad \text{in } \mathbb{R}^N \times \mathbb{R}^+. \tag{11}$$

In the particular case of a velocity in normal direction

$$V = v\mathbf{n} \quad \text{on } \Gamma \times \mathbb{R}^+, \tag{12}$$

we can use the relation  $\mathbf{n} = \frac{\nabla\phi}{|\nabla\phi|}$  to compute the evolution of the level set function from the nonlinear level set equation of Hamilton–Jacobi type

$$\frac{\partial\phi}{\partial t} + v |\nabla\phi| = 0, \quad \text{in } \mathbb{R}^N \times \mathbb{R}^+. \quad (13)$$

Note that for the formulation (13) the function  $v$  needs to be given on  $\mathbb{R}^N$  or at least on some neighborhood of  $\Gamma$  in  $\mathbb{R}^N$ . If  $v$  is a priori only on  $\Gamma$ , it has to be extended to  $\mathbb{R}^N - \Gamma$ . In general, evolutions with the same normal component of the velocity coincide (tangential components correspond to re-parametrizations only), so that we will restrict our attention to the case (12).

For a detailed exposition of level set methods for the propagation of interfaces we refer to the monograph by Osher and Fedkiw [24].

In principle, the level set method is capable to perform topology changes in the propagating shape. Especially merging components and breaking up of one component into two are typical topology changes which can be treated using the level set method. However, since the level set method is designed to describe the propagation of interfaces with a given speed function defined on the interface, it is usually not possible to create holes within existing shapes away from the boundary or to introduce new components of the shape at locations far from the boundary. For shape optimization problems this might cause the level set propagation to stop in local minima where local movement of the boundary cannot produce a decent of the cost function value but change of the topology (e.g. introduction of holes) might give further reduction of the cost function value. There are several situations where the disability of the level set method to create holes can in fact be observed. For example, in a one dimensional situation one can easily show that a simply connected domain will remain simply connected during the evolution. The propagation of zero-dimensional interfaces (isolated points) by one-dimensional level set functions might be a useful way to describe crack propagation, since a planar crack can be represented by a one-dimensional level set function defined on curve which again can be given as the zero level set of a two-dimensional level set function (cf. [30]). In the context of shape optimization, Allaire et al. [4] observed problems in creating holes in spatial dimension two and three. In any of these cases, a further decrease of the objective functional can be obtained by the nucleation of small holes, i.e., by perturbations of the shape in the  $L^1$ -topology. In order to realize this idea in a computational way, we propose a modification incorporating the topological derivative in the following section.

#### 4. Level set methods with topological derivatives

Due to the limited capability of the shape derivative based level set method to generate holes, it seems necessary to consider a modification, including a term dependent on the topological derivative. An obvious modification is to add a forcing term, in order to cause negative values of the level set function to increase if it is favourable to add a hole at this position and to decrease if not (vice versa for positive values). In accordance with the considerations in Section 3 this strategy results in a first-order Hamilton–Jacobi equation for the level set function, of the form (13)

$$\frac{\partial\phi}{\partial t} + F|\nabla\phi| + \omega G = 0, \quad (14)$$

with  $\omega$  being a positive real parameter controlling the influence of the additional source term  $G$ . The speed  $F$  will be chosen as a descent direction for the propagation of the zero level set of  $\phi$ .

It remains to choose the functions  $F$  and  $G$  in dependence of state, adjoint state and of the shape given by the zero level set of  $\phi$ . It seems reasonable to choose  $F$  in dependence of the shape derivative, since this term

determines the geometric motion, and  $G$  in dependence of the topological derivative, since the forcing term determines the nucleation of new holes. In the following we shall use the notation  $g(x, t) := d_{\mathcal{F}}J(\Omega(t))(x)$ .

We base the choice of the source term  $G$  on the following reasoning:

- If  $\phi(x, t) < 0$  and  $g(x, t) < 0$ , then it is favorable to create a hole at  $x$  and thus, the value of  $\phi$  should increase. Vice versa, if  $\phi(x, t) > 0$  and  $g(x, t) < 0$ , then the value of  $\phi$  should decrease, since it is favorable to add material.
- If  $\phi(x, t) < 0$  and  $g(x, t) > 0$ , then it is not favorable to create a hole and thus, the value of  $\phi$  should not increase. Vice versa, if  $\phi(x, t) > 0$  and  $g(x, t) > 0$ , then the value of  $\phi$  should not decrease.

The movement of the level set function towards zero if topology change appears favorable might not immediately (within one time-step) generate a topology change but it enables an eventual topology change away from the zero level set if the tendency towards changing the topology persists during several time-steps in the evolution of the level set function.

If we ignore the influence of the first-order term (which rather causes a horizontal than a vertical movement of the values of  $\phi$ ) for the moment, then the change in  $\phi$  is determined by

$$\frac{\partial \phi}{\partial t}(x, t) = -G(x, t). \tag{15}$$

Hence, from the above arguments we need that  $G$  satisfies

$$\begin{cases} G(x, t) > 0 & \text{if } \phi(x, t)g(x, t) > 0, \\ G(x, t) < 0 & \text{if } \phi(x, t)g(x, t) < 0. \end{cases} \tag{16}$$

It seems natural to choose  $G$  in linear dependence on  $g$ , such that the topological derivative has higher influence where it is more favorable to add holes. A linear dependence of  $G$  on the level set function  $\phi$  would be unnatural and might lead to unreasonable results, since then the increase of the level set function is slowed down when its values is close to zero. Therefore, we shall use the simple choice

$$G(x, t) = -\text{sgn } \phi(x, t)g(x, t), \tag{17}$$

which obviously meets the above requirements. For the model problem (1) and (2), this choice is particularly simple, since due to (10), we obtain that  $G = -w$ . Hence, the modified level set evolution is given by the first-order Hamilton–Jacobi equation

$$\frac{\partial \phi}{\partial t} - w(|\nabla \phi| + \omega) = 0. \tag{18}$$

We can give yet another, variational interpretation for the choice of the term  $G$ . We will present the arguments for the model problem (2), but the transfer to a more general situation is straight-forward. Suppose that we are given the optimal shape  $\Omega_o$  with respect to the cost functional (1). If  $x \in \Omega_o$ , that is  $\phi(x) < 0$ , changing the local properties from material to void, i.e., placing a hole at  $x$  must increase the value of the cost functional. Therefore  $d_{\mathcal{F}}(\Omega_o)(x) = -w(x) \geq 0$ . Hence,  $\phi(x)w(x) \geq 0$ . On the other hand, if  $x \in D - \overline{\Omega_o}$ , we have  $\phi(x) > 0$ . Adding material at  $x$  cannot decrease the cost function value and we obtain  $d_{\mathcal{F}}(\Omega_o)(x) = w(x) \geq 0$ , from which we conclude again that  $\phi(x)w(x) \geq 0$ . Obviously, if  $x \in \partial\Omega_o$  then  $\phi(x) = 0$  and also  $\phi(x)w(x) \geq 0$ . In other words, for the optimal shape the product  $\phi w$  is nonnegative. Adding a term

$$K(\phi) = -\omega \int_D \phi w \, dx \tag{19}$$

to the cost functional (1) will enforce the matching of the signs of  $\phi$  and  $w$  on  $D$  as the minimization proceeds. The derivative of  $K$  with respect to the shape encoded in  $\phi$  is given by  $\frac{\partial K}{\partial \phi} = -\omega w$  which leads to



the gradient flow (18) for the functional  $\hat{J}(\Omega, \phi) = J(\Omega) + K(\phi)$ . Note that  $\hat{J}$  does not have a minimizer since  $\hat{J}$  is not bounded from below in the variable  $\phi$ . This means also that the gradient flow (18) does not converge to a steady state for the level set function  $\phi$ . This, however, is not a problem since we are interested only in the shape variable  $\Gamma = \partial\Omega$ , i.e. the zero level set of  $\phi$  which in fact becomes stationary at the solution to (1) even though the values of  $\phi(\cdot, t)$  may still change (but not their sign). Let us consider the influence of the new forcing term in more detail. Suppose we are given a point  $x \in D - \Gamma$  at which the signs of  $\phi$  and  $w$  do not match. Then the term  $-\omega w$  will drive  $\phi$  towards zero, eventually leading to a change in the geometry of  $\Omega$ . If, however, the signs of  $\phi$  and  $w$  already agree, the movement induced by  $-\omega w$  will push  $\phi$  even further away from zero thus leaving  $\Omega$  unchanged.

## 5. Numerical experiments

In the following we present the results of some numerical experiments, which demonstrate the improvement that can be achieved by using the topological derivative in addition to the shape derivative. We performed two tests for the model problem (2), the first in one spatial dimension, where the original level set method can never split, and a second in two spatial dimensions, with an obstacle including a hole. All algorithms have been implemented in the software system MATLAB.

### 5.1. A one-dimensional example

We start with a simple one-dimensional example related to model problem (2). The exact solution in this case consists of two connected components, while the initial value for the level set method consists of a single connected component only. The indicator functions of the exact solution (left) and the initial shape (right) are shown in Fig. 1.

Both the level set equation and the elliptic state equation are discretized on a uniform grid with 128 points. We use a standard finite difference scheme for the elliptic equation and a simple first-order monotone scheme for the level set equation (cf. [24] for details). The time step  $\tau$  is chosen according to the CFL-condition, i.e., at time  $t_j$

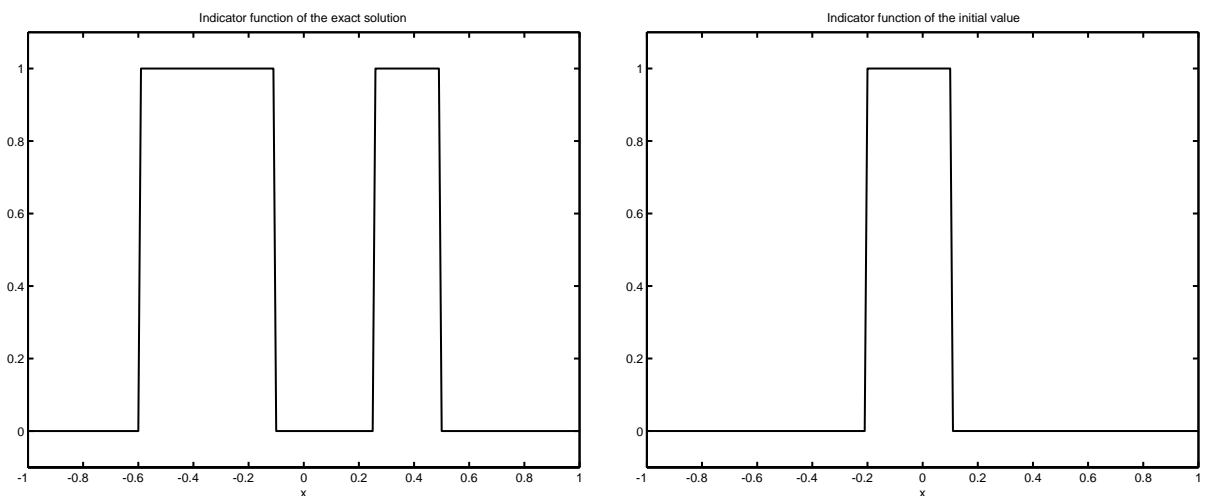


Fig. 1. Exact solution (left) and initial value (right) in Example 1.

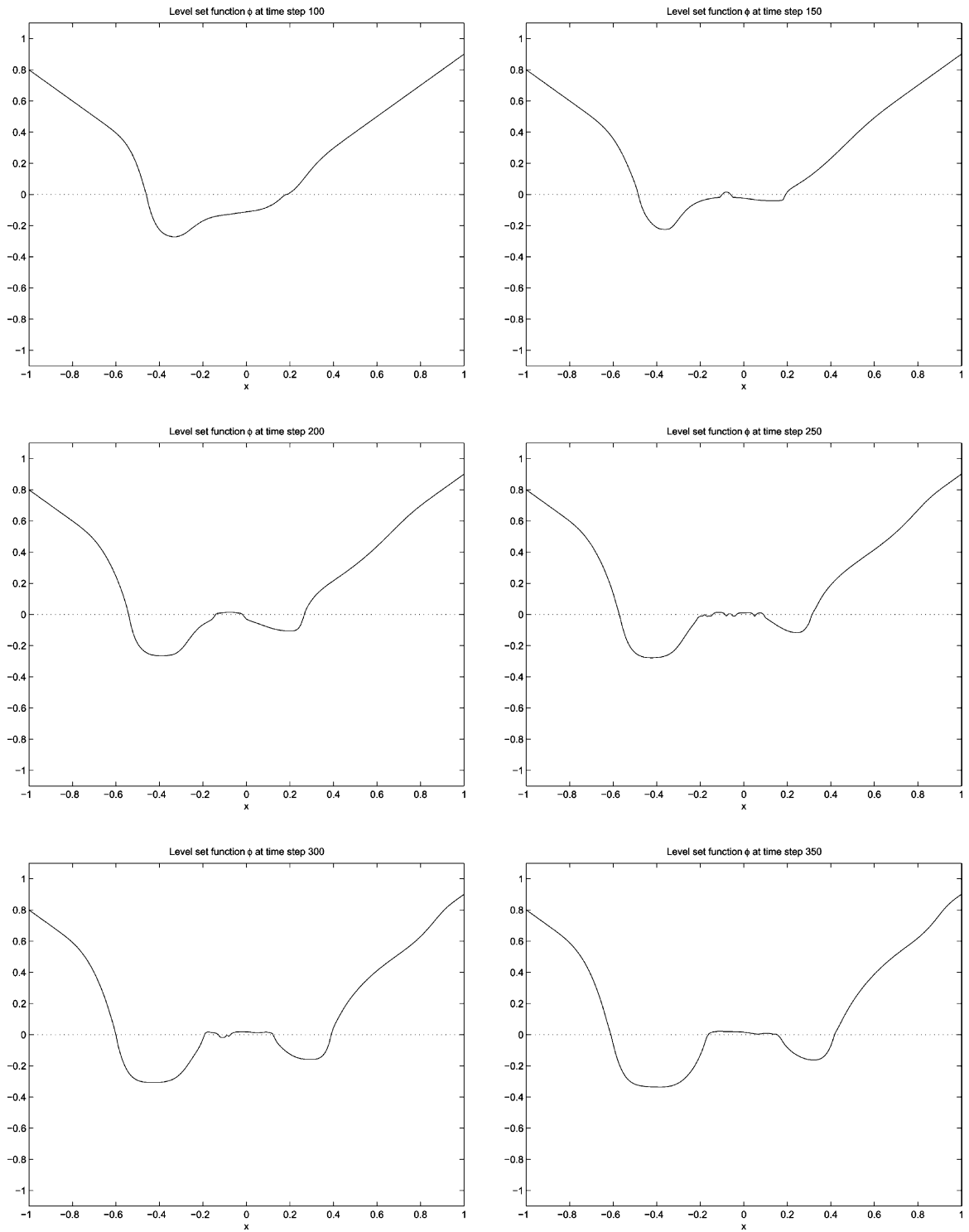


Fig. 2. Evolution of the level set function at time steps 100, 150, 200, 250, 300, and 350.

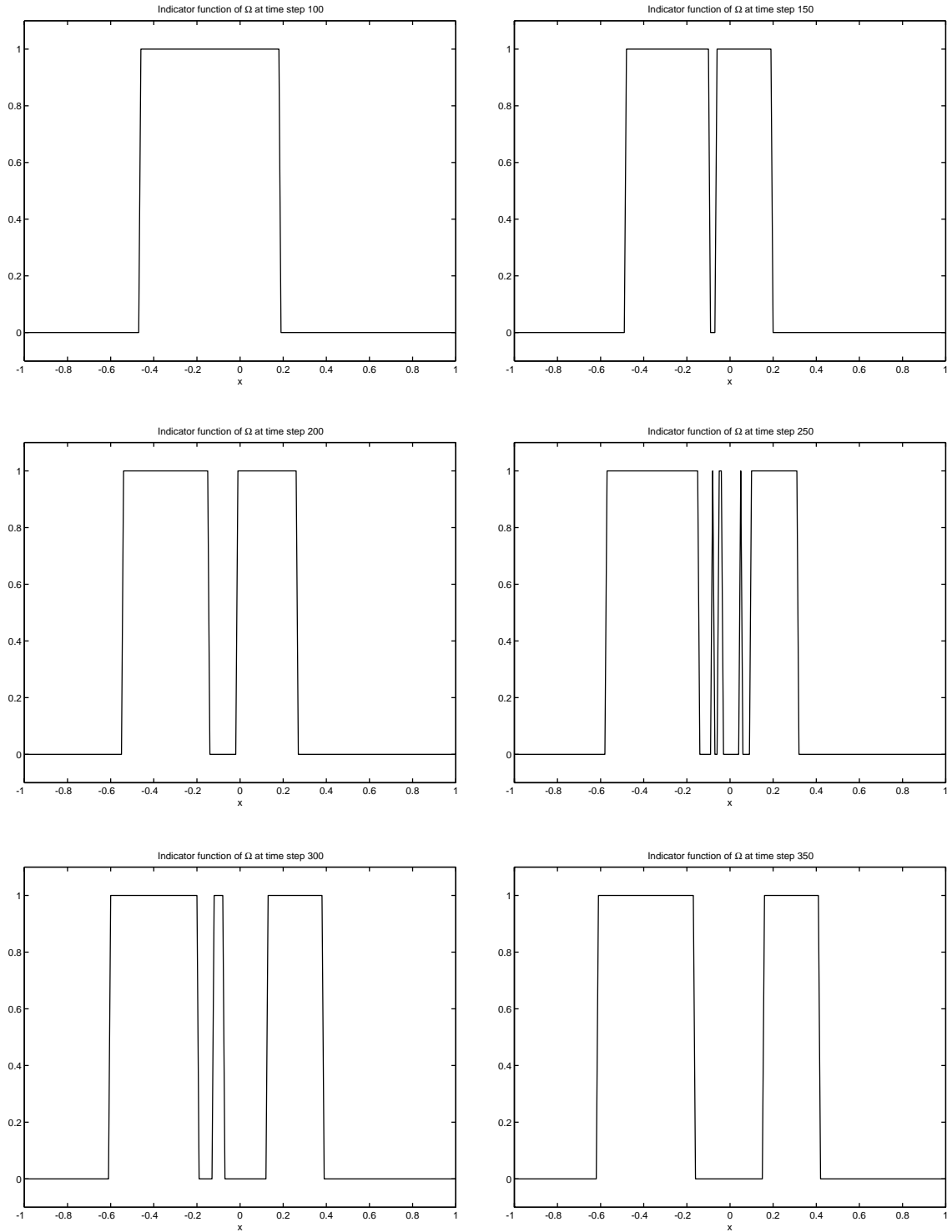


Fig. 3. Evolution of the indicator function at time steps 100, 150, 200, 250, 300, and 350.

$$\tau = 0.9 \frac{h}{\max_x F(x, t_j)}, \tag{20}$$

where  $h = 1/127$  is the fineness of the spatial discretization. This choice ensures the stability of the explicit discretization method for the level set equation (cf. [24]). As a starting value for the level set function we used the signed distance function of the initial shape shown in Fig. 1.

For  $\omega = 1$ , the evolution of the level set function and the corresponding indicator function for the zero level set are illustrated in Figs. 2 and 3 by plots after time steps 100, 150, . . . , 350. One observes that at the initial stage of the evolution, the geometric motion forced by the shape derivative is dominating and the shape evolves toward the convex envelope of the two obstacles in the exact solution. We want to mention at this point that this effect is not particular for the (narrow) initial value we used, it also occurred for different initial values. For example, for an initial value including the convex envelope of the two obstacles, the motion was decreasing the size at the initial stage. With decreasing normal speed in the geometric motion, the topological derivative becomes more and more important and changes the shape of the level set function. As one would expect in this example, the largest value for the topological derivative is attained where the exact solution actually has a hole. Note that the signed distance function of the initial value takes its minimal value in the hole in the exact solution. Therefore it is particularly difficult in this case to generate a hole at the right location. Nonetheless, the proposed level set evolution succeeds to generate the hole.

In Fig. 4, plots of the residual and of the  $L^1$ -difference in the indicator functions of the evolving shape and the exact solution are plotted versus the number of time steps, both for the original level set approach based on the speed method and for the modification incorporating the topological derivative. One observes that the original approach stagnates and is not able to compute the exact solution as expected, while the modified method decreases both the residual and the  $L^1$ -error to zero.

The results for different choices of the parameter  $\omega$  are shown in Fig. 5. One observes that the decrease in the error and objective is faster for higher values of  $\omega$ , which is to be expected, since the nucleation occurs earlier. Nonetheless, the decrease is slower in a subsequent phase for a very large value ( $\omega = 10$ ), mainly due to the nucleation of other holes, which then have to be removed by the geometric motion. One observes that the number of time steps needed for  $\omega = 1$  and  $\omega = 10$  in order to decrease the error to the limiting value at this discretization is quite the same, while the evolution is slower for  $\omega = 0.1$ .

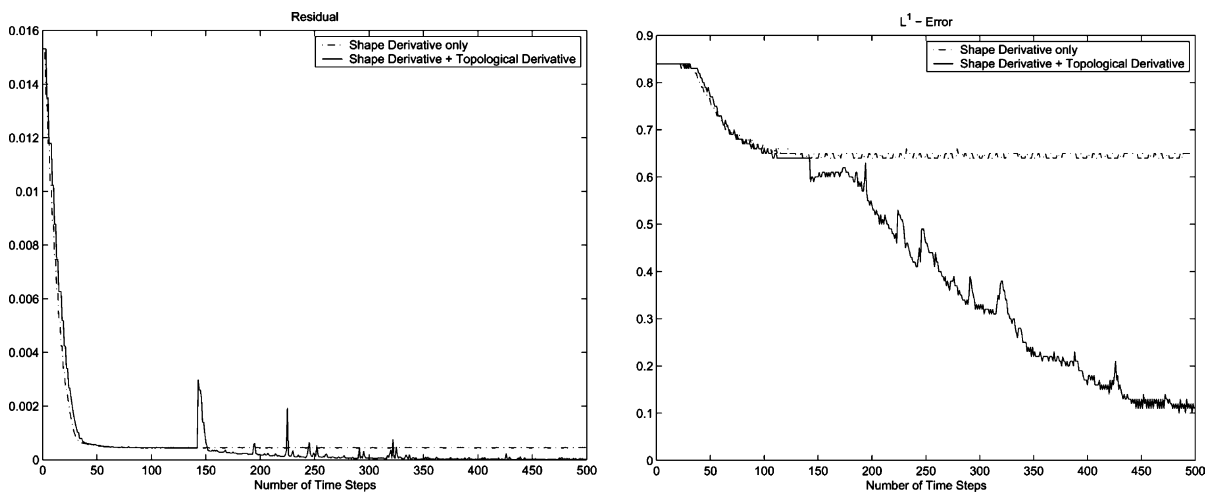


Fig. 4. Residual (left) and error in the  $L^1$ -norm (right) vs. number of time steps, for the original level set method using the shape derivative only (dash-dotted) and with the additional topological derivative (solid).

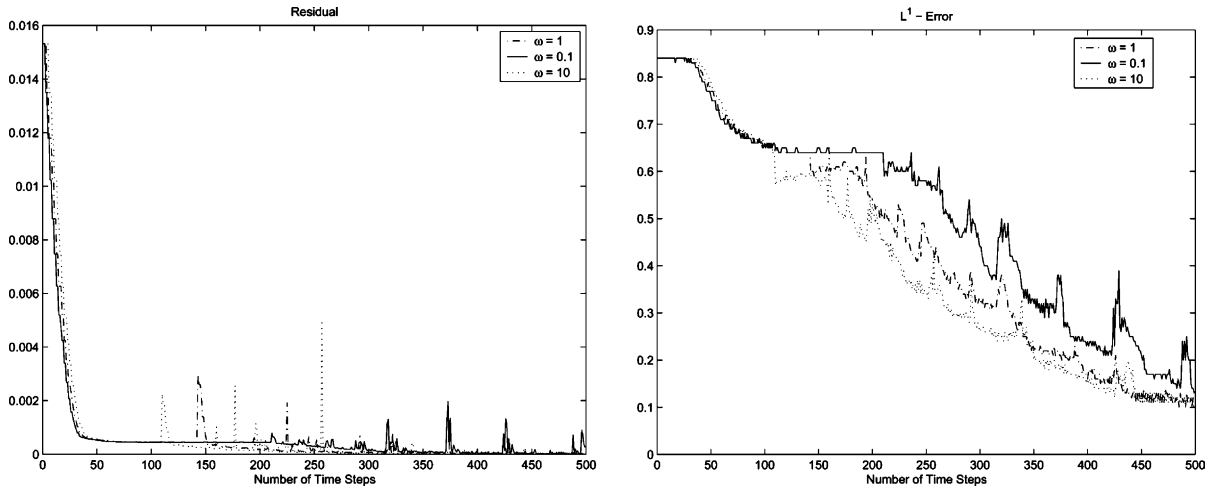


Fig. 5. Residual (left) and error in the  $L^1$ -norm (right) vs. number of time steps, with different weighting parameters  $\omega = 1$  (dash-dotted),  $\omega = 0.1$  (solid), and  $\omega = 10$  (dotted).

One also observes that more than a single hole are generated during the evolution (see time steps 200, 250 to 300), but finally one obtains the correct number of holes. In addition, the objective functional is not strictly decreasing during the evolution, but shows some small increases, which are compensated by larger decreases in the following time steps. Such fluctuations in the number of holes and in the objective functional can be caused by several reasons:

- If the parameter  $\omega$  is too small, the level set function tends to become rather flat around zero. Therefore, small oscillations will cause new holes, which is obviously undesirable.
- If the parameter  $\omega$  is too large, then the level set function becomes very steep (almost discontinuous) around a new hole and thus it is difficult to control numerical oscillations in the level set except with higher artificial diffusion (e.g. in a Lax–Friedrichs scheme). Moreover, the topological derivative has a very strong effect also while the geometric motion is still significant and therefore it is not clear if the energy is monotonously increasing.
- An increase in the objective functional also happens for level set methods without topological derivatives if the time step is chosen proportional to the CFL-bound (cf. [5,9]), which is mainly due to the fact that this time is too large to achieve a decrease in the objective functional. A step-size control could help to overcome this difficulty, but it might also slow down the algorithm by limiting the time step too severely. Numerical experience shows that usually an increase in the objective is followed by a stronger decrease, which allows to obtain convergence within few time steps.

In order to overcome the problems noted above, we also investigated a modification of our approach, with a constant  $\omega_k$  dependent on the time step. We choose

$$\omega_k = \begin{cases} 1 & \text{if } J(\Omega_{k-1}) - J(\Omega_{k-2}) > -\epsilon, \\ 0 & \text{else,} \end{cases} \quad (21)$$

i.e., we incorporate the topological derivative only if there is not sufficient descent in the objective. For the numerical simulation we chose  $\epsilon = 10^{-4}$ . A second modification we considered, was to switch also the term based on the shape derivative, i.e., the evolution in time step  $k$  is given

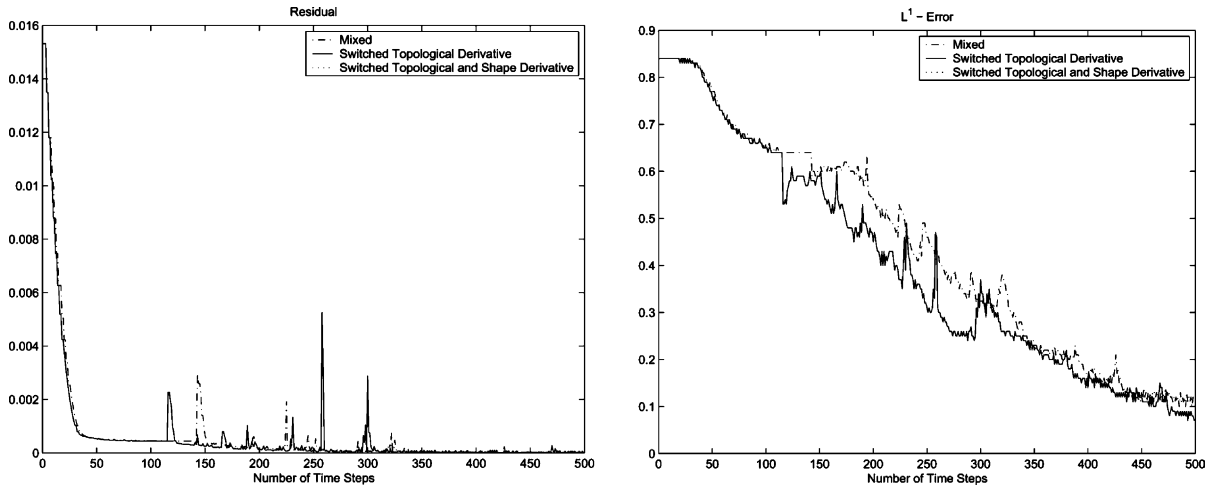


Fig. 6. Residual (left) and error in the  $L^1$ -norm (right) vs. number of time steps, using the mixed evolution (dash-dotted), switching in the topological derivative (solid), and switching in both derivatives (dotted).

$$\frac{\partial \phi}{\partial t} = \begin{cases} -G(\phi) & \text{if } J(\Omega_{k-1}) - J(\Omega_{k-2}) > -\epsilon, \\ -F |\nabla \phi| & \text{else.} \end{cases} \quad (22)$$

The result of these modifications is a clear distinction of the geometric motion and of nucleation. In this way less nucleation events happen.

A quantitative comparison of the modifications (21) (denoted ‘Switched Topological Derivative’) and (22) (denoted ‘Switched Topological and Shape Derivative’) to (14) (now for  $\omega = 1$ ) is shown in Fig. 6, where again the residual and the  $L^1$ -error are plotted vs. the number of time steps. One observes that the modifications improve the convergence speed with respect to (14), while there is little difference between (21) and (22). Since, in addition, the modifications yield an evolution with less nucleation events, it seems

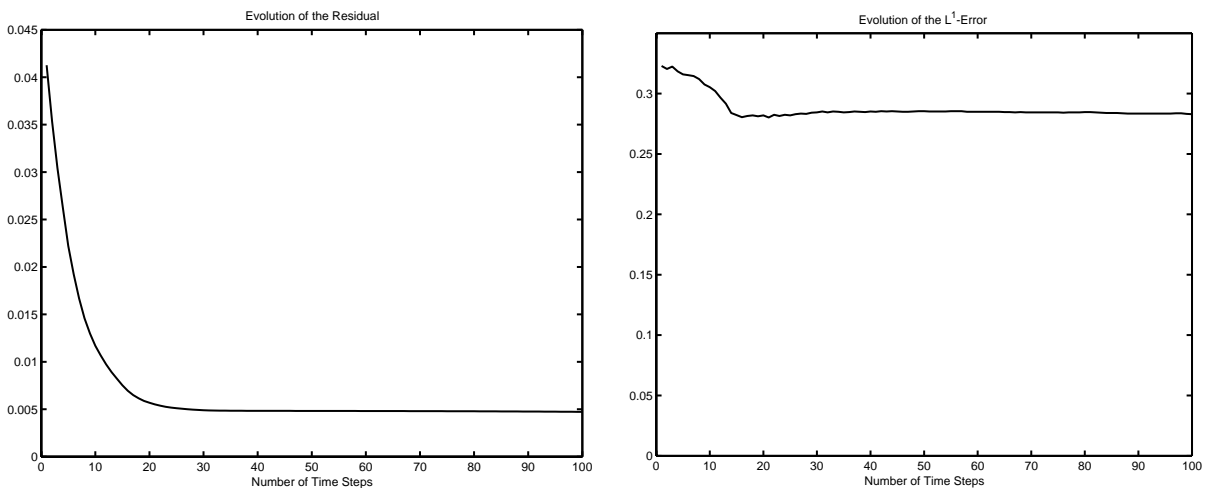


Fig. 7. Residual (left) and error in the  $L^1$ -norm (right) vs. number of time steps, using the level set evolution only.

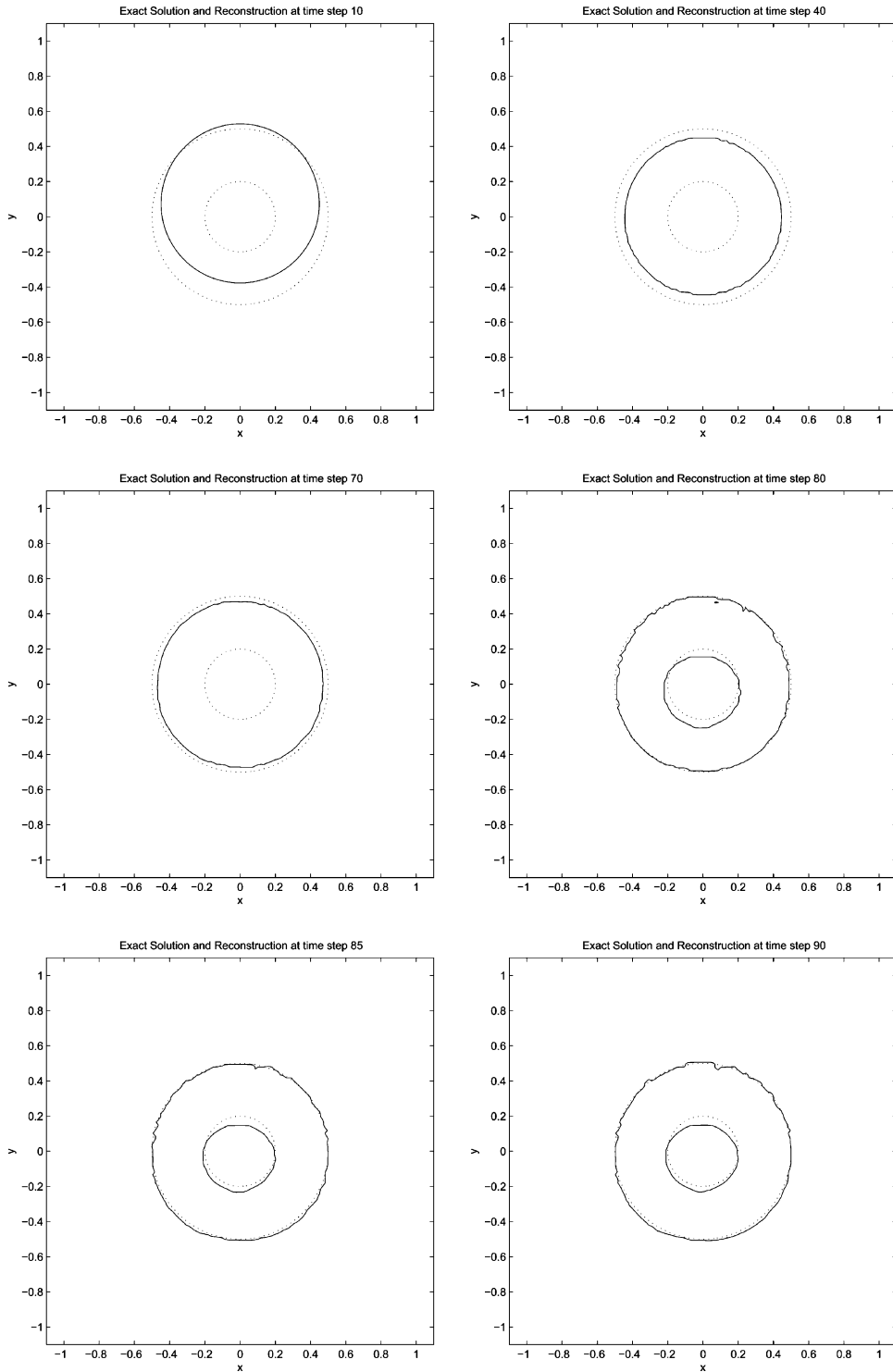


Fig. 8. Evolution of the shape at time steps 10, 40, 70, 80, 85, and 90.

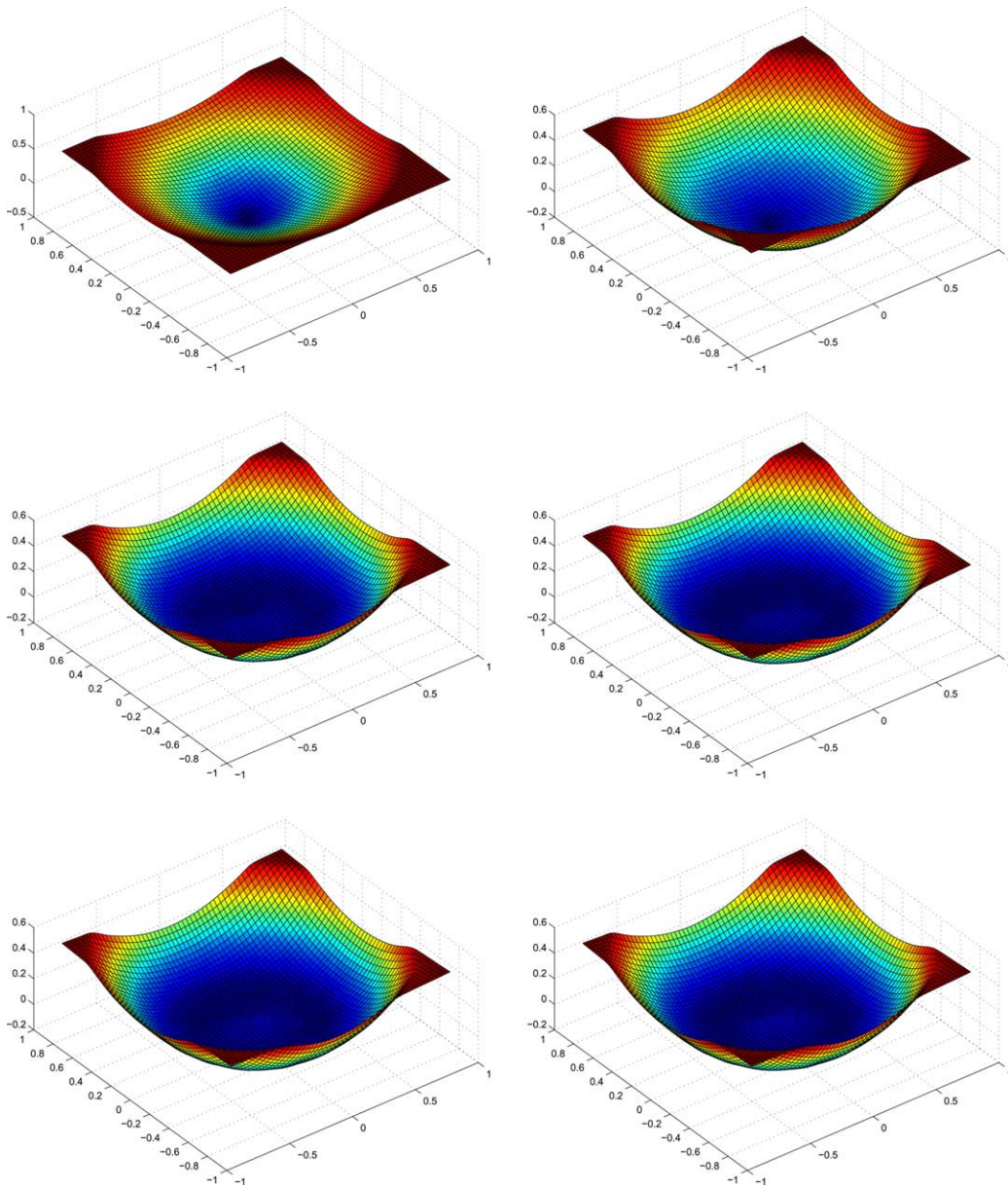


Fig. 9. Evolution of the level set function at time steps 10, 40, 70, 80, 85, and 90.

favorable to use one of the modifications for the numerical solution, as we will also do in our two-dimensional example in Section 5.2.

A final inspection of the results shows that probably the evolution of the level set function, but not the final result will depend on the choice of the initial value. If the initial value for  $\phi$  was chosen to be flat e.g. in the level set  $\{\phi \leq 0.1\}$ , then the first nucleation would obviously appear where the magnitude of the topological derivative has largest magnitude and the subsequent level set evolution might yield convergence to the exact solution without creation of further holes. In our case, with the signed distance function being the



initial value, another hole might nucleate first due to a larger initial value of the level set function. Note however, that the level set evolution we propose converges also in this difficult situation, which indicates that the final result is independent of the initial value.

### 5.2. A two-dimensional example

The two-dimensional example for (2) we consider is the reconstruction of an obstacle being a ball of radius 0.5 which includes a hole of radius 0.2, both centered at the origin. The computational domain is the unit square. We discretize the state and adjoint equation using piecewise linear finite elements (within the MATLAB PDE Toolbox) and the level set equation by finite differences on a square grid of  $64 \times 64$  points. For the numerical solution of the level set equation we use a weighted ENO-scheme (cf. [20]) of fifth order in space and third order in time, with a Godunov-type flux. The time step is chosen as in the one-dimensional example.

The initial value in our computation is a ball of radius 0.4 centered at the point  $x = -0.2, y = 0.3$ . The corresponding initial value for the level set function is the signed distance function to this ball. Due to the numerical experience in the one-dimensional example, we used the modification (21) to avoid a too large number of nucleation events during the level set evolution, again with  $\epsilon = 10^{-4}$ .

We start with a numerical experiment using the shape derivative only, which leads to a convergence of the shape to the outer contour of the exact solution. Note that in principle, this evolution could split up and create a hole, but it seems that the method is stopped in a stationary point with respect to normal variations of the shape. The nonconvergence of this approach is illustrated in Fig. 7, which shows a plot of the residual and the  $L^1$ -error versus the number of time steps, both clearly stagnating after few steps.

The evolution of the shape and the level set function are illustrated in Figs. 8 and 9 at different time steps. At the initial stage, which is a pure geometric motion ( $\omega = 0$ ), the shape converges to the outer contour of the obstacle until this motion stagnates. With the stagnation of the geometric motion, the topological derivative is activated ( $\omega = 1$ ), which leads to a nucleation event after around 75 time steps. Since this leads to a significant decrease in the objective, the topological derivative is deactivated again ( $\omega = 0$ ), and the inner contour converges via pure geometric motion to the exact shape. Finally, this geometric motion stagnates again, which means that the topological derivative would have to be activated, but since no further nucleation is favorable at this point, the sign of the topological derivative is such that no new holes

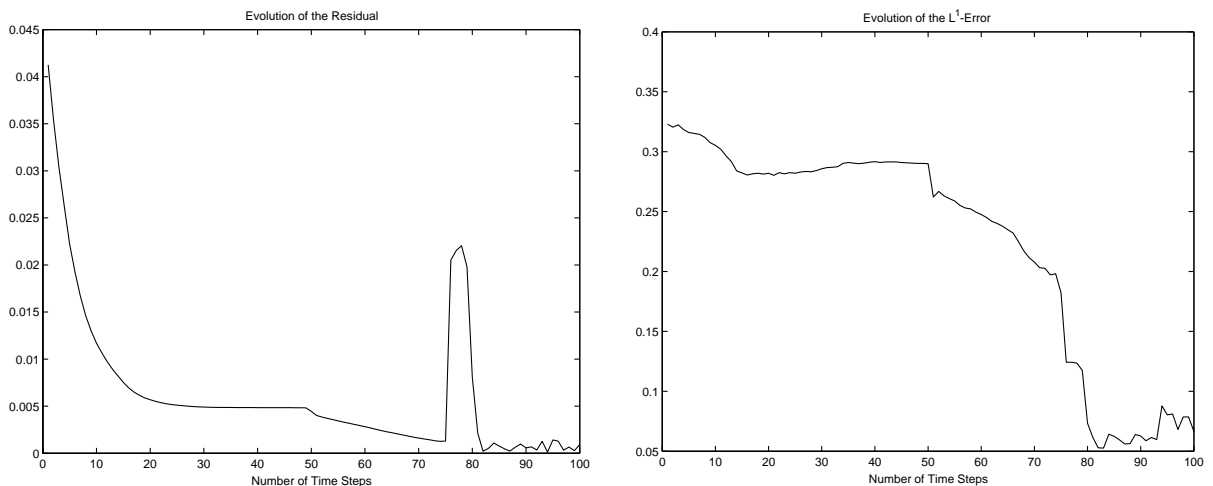


Fig. 10. Residual (left) and error in the  $L^1$ -norm (right) vs. number of time steps.

can be created and therefore the evolution has to be stopped. From the evolution of the level set function one observes that the topological derivative has almost no effect except around the origin, where a new hole is created.

Finally, we show the evolution of the residual and the  $L^1$ -error in time in Fig. 10. The residual stagnates rather early and the topological derivative is activated after around 45 time steps, leading to a nucleation at time step 75. Surprisingly, the objective is decreasing already before the nucleation event occurs. This might be due to the fact that the level set function changes locally around the exterior contour. Note that the error is decreasing slower than the objective at this stage. Another unexpected effect is an increase in the objective right after nucleation. This is probably due to the fact that a rather large object nucleates in this case (the level set function is very flat in a rather larger region around the origin), and hence the asymptotic in the topological derivative is not valid. Nonetheless, this increase in the objective yields a stronger increase almost to zero in subsequent time steps and a strong decrease of the error. One also observes that the objective functional and the error oscillate and increase after a minimum is reached after around 82 time steps. This is a typical effect for ill-posed problems in presence of noise and indicates that the iteration should be stopped at this stage. We want to mention that the noise in our numerical examples arises from numerical errors only, for a further investigation of the effects of data noise we refer to future work.

## References

- [1] R.A. Adams, Sobolev Spaces, Academic Press, New-York, 1975.
- [2] G. Allaire, Shape optimization by the homogenization method, Springer-Verlag, New York, 2002.
- [3] G. Allaire, F. Jouve, A.M. Toader, A level-set method for shape optimization, C.R. Acad. Sci. Paris Ser. I 334 (2002) 1125–1130.
- [4] G. Allaire, F. Jouve, A.M. Toader, Structural optimization using sensitivity analysis and a level-set method, Preprint (CMAP École Polytechnique, Paris, 2003).
- [5] H. Benameur, M. Burger, B. Hackl, Level set methods for geometric inverse problems in linear elasticity, Preprint, 2003.
- [6] M.P. Bendsoe, O. Sigmund, Topology Optimization, Springer, Berlin, 2002.
- [7] B. Bourdin, A. Chambolle, Design-dependent loads in topology optimization, ESAIM Control Optim. Calc. Var. 9 (2003) 19–48.
- [8] M. Burger, A level set method for inverse problems, Inverse Problems 17 (2001) 1327–1356.
- [9] M. Burger, A framework for the construction of level set methods for shape optimization and reconstruction, Interfaces and Free Boundaries 5 (2003) 301–329.
- [10] M.C. Delfour, J.P. Zolésio, Shapes and Geometries. Analysis, Differential Calculus, and Optimization, SIAM, Philadelphia, 2001.
- [11] O. Dorn, E.M. Miller, C.M. Rappaport, A shape reconstruction method for electromagnetic tomography using adjoint fields and level sets, Inverse Problems 16 (2000) 1119–1156.
- [12] O. Dorn, Shape reconstruction in 2D from limited-view multifrequency electromagnetic data, Preprint, 2000.
- [13] S. Garreau, P. Guillaume, M. Masmoudi, The topological asymptotic for PDE systems: the elasticity case, SIAM J. Control Optim. 39 (2001) 1756–1778.
- [14] M. Giaquinta, Introduction to Regularity Theory for Nonlinear Elliptic Systems, Birkhäuser, Basel, 1993.
- [15] P. Guillaume, K. Sid Idris, The topological asymptotic expansion for the dirichlet problem, SIAM J. Control Optim. 41 (2002) 1042–1072.
- [16] F. Hettlich, W. Rundell, Iterative methods for the reconstruction of an inverse potential problem, Inverse Problems 12 (1996) 251–266.
- [17] M. Hintermüller, W. Ring, A second order shape optimization approach for image segmentation, SIAM J. Appl. Math., in press.
- [18] M. Hintermüller, W. Ring, An inexact Newton-CG-type active contour approach for the minimization of the Mumford-Shah functional, J. Math. Imag. Vision 20 (2003) in press.
- [19] K. Ito, K. Kunisch, Z. Li, Level-set function approach to an inverse interface problem, Inverse Problems 17 (2001) 1225–1242.
- [20] G.S. Jiang, D. Peng, Weighted ENO-schemes for Hamilton–Jacobi equations, SIAM J. Sci. Comput. 21 (2000) 2126–2143.
- [21] A. Litman, D. Lesselier, F. Santosa, Reconstruction of a two-dimensional binary obstacle by controlled evolution of a level-set, Inverse Problems 14 (1998) 685–706.
- [22] S. Osher, F. Santosa, Level set methods for optimization problems involving geometry and constraints. I. Frequencies of a two-density inhomogeneous drum, J. Comput. Phys. 171 (2001) 272–288.
- [23] S. Osher, J.A. Sethian, Fronts propagating with curvature-dependent speed: algorithms based on Hamilton–Jacobi formulations, J. Comput. Phys. 79 (1988) 12–49.

- [24] S. Osher, R.P. Fedkiw, *The Level Set Method and Dynamic Implicit Surfaces*, Springer, New York, 2002.
- [25] F. Santosa, A level-set approach for inverse problems involving obstacles, *ESAIM: Control, Optimisation Calculus Variations* 1 (1996) 17–33.
- [26] A. Schumacher, *Topologieoptimierung von Bauteilstrukturen unter Verwendung von Lochpositionierungskriterien*, PhD Thesis, Universität-Gesamthochschule-Siegen, 1995.
- [27] J. Sokolowski, A. Żochowski, On the topological derivative in shape optimization, *SIAM J. Control Optim.* 37 (1999) 1251–1272.
- [28] J. Sokolowski, A. Żochowski, Topological derivatives for elliptic problems, *Inverse Problems* 15 (1999) 123–134.
- [29] J. Sokolowski, J.P. Zolesio, *Introduction to Shape Optimization*, Springer, Berlin, 1992.
- [30] M. Stolarska, D.L. Chopp, N. Moes, T. Belytschko, Modelling crack growth by level sets in the extended finite element method, *Int. J. Numer. Meth. Eng.* 51 (2001) 943–960.
- [31] J.P. Zolesio, The material derivative (or speed) method for shape optimization, in: *Optimization of Distributed Parameter Structures*, vol. II, NATO Adv. Study Inst. Ser. E, Appl. Sci. 50 (1981) 1089–1151.